Regular Article

INORGANIC CHEMISTRY RESEARCH
Published by the
Iranian Chemical Society
www.inorgchemres.org
info@inorgchemres.org

Inorg. Chem. Res., Vol. 4, No. 2, 279-294, December 2020
DOI: 10.22036/icr.2020.240977.1081

Nano structured Mercury(II) Schiff Base Complexes of a N_3-Tridentate Ligand as New Biological Active Agents

Sara Khani[a], Morteza Montazerozohori[a,*], Reza Naghiha[b] and Shiva Joohari[c]

[a]*Department of Chemistry, Yasouj University, Yasouj, 7591874831, Iran*
[b]*Department of Animal Sciences, Faculty of Agriculture, Yasouj University, Yasouj, Iran*
[c]*Department of Basic Sciences, Yasooj Branch, Islamic Azad University, Yasooj, Iran*
(Received 24 July 2020, Accepted 12 November 2020)

In this study, a N_3-Schiff base ligand (L) was obtained from *via* condensation reaction of diethylenetriamine and (Z)-3-(4-(dimethylamino)phenyl)acrylaldehyde (1:2 ratio). Then some its new five coordinated $HgLX_2$ complexes inwhich X is halide/pseudohalide were synthesized. The ligand and its complexes were characterized by various analysis tools such as FT-IR, ^{1}H and ^{13}C NMR, UV-Vis, thermal analyses and molar conductivity measurements. Based on the spectral data and conductivity measurements, all the newly prepared compounds were found to be non-electrolyte. Moreover some mercury complexes were prepared in nano-structured size by sonochemical method that confirmed by X-ray powder diffraction method (XRD) and scanning electron microscopy (SEM) analyses. The Schiff base and its mercury complexes have been screened for their *in vitro* antibacterial activities (*Escherichia coli*, *Staphylococcus aureus*, *Pseudomonas aeruginosa* and *Bacillus subtilis*) and antifungal activities (*Candida albicans* and *Aspergillus oryzae*) using well diffusion method. Furthermore, thermal behaviors of the ligand and its mercury complexes were evaluated in the range of room temperature to 1000 °C under nitrogen atmosphere. The results showed that Schiff base ligand and its complexes were decomposed completely *via* 2 to 5 steps.

Keywords: Schiff base, Nano-structured, Mercury, Antibacterial, Antifungal, XRD, SEM

INTRODUCTION

Schiff bases are a group of organic compounds with a characteristic functional group (-RC=N-). Schiff bases have considerable importance in inorganic and organometallic chemistry; and because of easy availability of iminic nitrogens, they are used as ligand in transition metal chemistry. An important class of Schiff base ligands in the coordination chemistry is Schiff bases which contain cinnamaldehyde sections [1-3]. Research on inorgaic complexes is fast developing because of their attractive electronic, chemical, catalysis and biological properties [4-8]. For instance, metal organic complexes are used as catalysts, pigments, dyes, polymer stabilizers, and intermediates in organic synthesis [9]. Biological activities such as acting as antimicrobial, antifungal, catechol oxidase, anti-HIV, DNA cleavage systems, anti-inflammatory, tumour growth inhibitors, biomimetic enzyme models and anticancer are a part of important properties of coordination compounds [10-19]. Even though metal-based antimicrobials have intense effects in microbial growth inhibition, their potential for toxicity in human beings confines their current application [20]. Organic molecules cannot perform some cellular functions, while they can be accomplished by metals that are indispensable for the biochemistry of life in all organisms. On the other hand, overdose of these essential metals can lead to deadline of the cells. In inorganic chemistry and biochemistry areas, group 12 metal ions with d^{10} electronic configuration have attracted a lot of attentions due to their varieties of coordination numbers, toxic environmental effects, mobilization and immobilization in the environment, molecular and crystalline aggregates

*Corresponding author. E-mail: mmzohory@yahoo.com

emanating from its d^{10} electronic [21-24]. Recently because of their antimicrobial activities, mercury complexes have been widely investigated [3,25,26]. Furthermore, a sensible agent for expansion chemistry of mercury(II) may be due to its extraordinarily toxicity to most of bacteria, yeast and microbicidal exceptional performance at low concentrations [27,28]. Depending on the different chemical forms of Hg, amount and exposure, the toxicity of mercury is altered [29,30]. Organo-mercurial complexes are used as antimicrobials, antiseptics, disinfectants and preservatives in pharmaceuticals.

Nowadays, sonochemical method is a common pathway for preparation of nanostructured compounds. In this method, irradiation of ultrasound waves to chemical reactions and processes is occurred. In fact, the sonochemical effect is the phenomenon of acoustic cavitation in reaction mixture. Cavitation is the formation, growth, and implosive collapse of bubbles in a liquid. Cavitational collapse produces intense local heating (~5000 K), high pressures (~1000 atm), and enormous heating and cooling rates (>109 K s^{-1}) and liquid jet streams (~400 km h^{-1}). These local high temperature and pressure cause increase in reaction speed, output, switching of reaction pathway, the reactivity of reagents and improvement of particle synthesis coating of nanoparticles.

With this background and in continuation of our previous work on the synthesis and properties of Schiff base complexes [25,31-35], herein we report the synthesis and characterization of some new mercury Schiff base complexes. The synthesized complexes were characterized by different spectroscopic and analytical techniques. Their potential as antimicrobial agents in growth inhibitory against microorganisms were sceened *in vitro* against some fungal and Gram positive and negative bacterial strains. Moreover thermal behavior and some thermokinetic activation parameters *via* their thermal decomposition steps of them were evaluated.

EXPERIMENTAL

Materials and Methods

All the reagents and solvents used in this work were provided from Aldrich and/or Merck chemical companies and used without any further purification. Chemicals and solvents including 4-dimethylaminocinnamaldehyde, diethylenetriamine, mercury(II) salts, ethanol, methanol, dimethylsulfoxide and dimethylformamide were used in this research. Mercury(II) thiocyanate or azide salts were prepared according to our previous report [35,36]. For biological tests, the solid medium of nutrient agar (Merck, Germany) was used for preparing the nutrient plates while Mueller Hinton broth (Scharlab) was applied as the liquid culture media. Sabouraub dextrose agar (Oxoid, Hampshire, England) was used as solid media for preparing the plates in antifungal studies. FT-IR spectra of the Schiff base ligand and its complexes were recorded on the FT/IR-JASCO-680 model instrument in the range of 400-4000 cm^{-1} using KBr disks. A JASCO-V570 spectrophotometer instrument was applied in the range of 200-800 nm for recording UV-Vis spectra of the compounds in DMF solution. ^{1}H and ^{13}C NMR spectra were recorded by use of a Brucker DPX FTNMR spectrometer at 300 MHz in DMSO-d6 solvent using TMS as internal standard. Melting points or decomposition temperature (°C) of the compounds was recorded by a Kruss instrument. Molar conductance measurement of the Schiff base ligand and its mercury complexes were taken in DMF solution (1.0×10^{-3} M) by using of a Jenway 4510 conductometer at room temperature. TG/DTA/DTG diagrams of the compounds have been investigated by use of a TGA instrument of Perkin-Elmer Pyris 60 Hz model in the range of room temperature to 1000 °C under nitrogen gas. SEM images of the nanostructured compounds were taken on a Philips XL30 field emission scanning electron microscope using Ac voltage of 20 kV. XRD patterns of some mercury complexes were recorded by a STOE type STIDY-MPGermany X-ray diffractometer with Cu Ka radiation (k = 1.5418 Å).

Synthesis of Schiff Base Ligand (L)

The synthesis of the Schiff base ligand was carried out similar to general procedure illustrated in our previous reports *via* a condensation reaction between diethylenetriamine and 4,4-dimethylaminocinnamaldehyde with 1:2 molar ratio in ethanol under vigorous stirring at room temperature [32]. After 5 h, the Schiff base ligand was

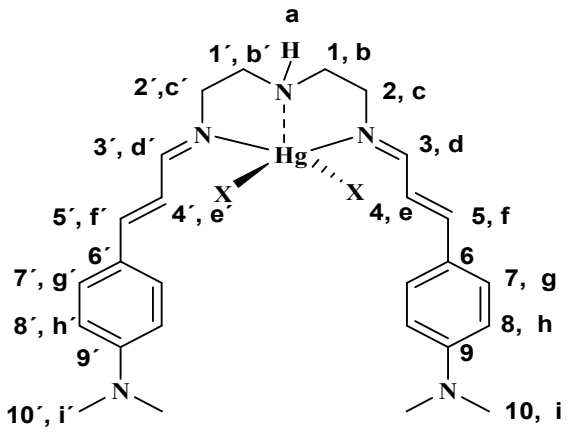

Scheme 1. Structural formula of the ligand and its mercury complexes (X = Cl^-, Br^-, I^-, SCN^-, N_3^-)

obtained as a yellow precipitate. Yield: 87%. M.p.: 117-121 °C. Physical and spectral data (IR, UV-Vis and NMR) of the ligand and its mercury complexes based on Scheme 1 and 2 are found in Tables 1, 2, 3 and 4.

Synthesis of Mercury(II) Complexes

Similarly like with our previous synthetic method, the mercury complexes were synthesized by stepwise addition of ethanolic solution of the ligand to the same moles of mercury salts in an ethanol solvent [35,37,38]. After complete addition, the reaction mixtures were vigorously stirred at room temperature for 4-5 h. The reaction products as precipitate were filtered and then washed twice with ethanol and dried at room temperature. Physical and spectral data (IR, UV-Vis and NMR) of the mercury complexes based on Scheme 1 and 2 are found in Tables 1, 2, 3 and 4.

Synthesis of Nano-structured Mercury Complexes

Nanostructured mercury complexes were prepared in a similar method for synthesis of bulk mercury complex but under sonication in an ultrasonic bath for about 1 h (Scheme 2). The obtained product was collected from the solution by filtration, and then washed with ethanol and dried at room temperature. The nano-structured mercury complexes were characterized by XRD and SEM techniques.

Antimicrobial Activity (*in vitro*)

The antimicrobial potential of the synthesized compounds were evaluated against four bacteria including *E. coli* and *P. aeruginosa* as Gram negative bacterial species; *Staphylococcus aureus* and *Bacillus subtilis* as Gram positive bacterial species using nutrient agar as medium (NA) and also, two fungal species including *Aspergillus oryzae* and *Candida albicans* on Sabouraud Dextrose Agar (SDA) medium by well diffusion method. In this method, the wells were dug in the media by using of a sterile borer [39]. The antimicrobial activity of each compound was confirmed by measurement of the zone diameter of inhibition of growth by well diffusion method. In well diffusion method that was used for antimicrobial studies, the concentrations of 15 and 7.5 and 3.75 mg mL^{-1} of the test samples were prepared in DMSO solvent. DMSO as solvent did not show notable antimicrobial effect alone against the selected bacteria and funguses. The wells on the agar medium were filled with the test samples and have been inoculated with pathogenic bacteria and funguses. After incubation of the resulting plates at 37 °C for 24 h, the diameter of the inhibition zone (mm) around each well on the the Petri dishes were measured as antimicrobial activity.

RESULTS AND CONCLUSION

Physical Properties and Analytical Data

In this report, some new mononuclear complexes of

Table 1. Analytical and Physical Data of the Schiff Base Ligand and its Hg(II) Complexes

Compound	Color	Dec. P. (°C)	Yield (%)	Λ°_{M} ($cm^2\ \Omega^{-1}\ M^{-1}$)
Ligand	Yellow	117-121 (M.P.)	87	21.7
$HgLCl_2$	Orange	158-163	88	13.56
$HgLBr_2$	Orange	152-157	91	23.90
$HgLI_2$	Orange	148-152	87	23.10
$HgL(SCN)_2$	Yellow	151-163	76	23.00
$HgL(N_3)_2$	Dark yellow	169-173	54	23.20

Dec. P. refers to decomposition temperature of compound. Λ°_{M} refers to Molar conductance. M. P. refers to melting point.

Table 2. Vibrational and Electronic Spectral Data of the Schiff Base Ligand and its Mmercury(II) Complexes

Compound	$\nu(NH)_{amine}$	$\nu(CH)_{alkene}$	$\nu(CH)_{aliph.}$	$\nu(CH)_{imine}$	ν(SCN/N3)	ν(C=N)	ν(C=C)	ν(C-N)	ν(M-N)	λ (nm), ε ($M^{-1}\ cm^{-1}$)
Ligand	3299	3028	2918	2881, 2803	-	1603	1460, 1442	1161	-	335(38800)
$HgLCl_2$	3213	3035	2910	2902, 2860	-	1593	1485, 1433	1161	447	383(15500), 465(47000)
$HgLBr_2$	3240	3033	2956	2918, 2854	-	1595	1481, 1433	1161	442	382(36500), 466(26500)
$HgLI_2$	3271	3087	2996	2910, 2859	-	1591	1483, 1433	1163	449	382(36500), 467(20000)
$HgL(SCN)_2$	3247	3082	2991	2863, 2804	2107	1593	1485, 1435	1163	449	381(33500), 466(28000)
$HgL(N_3)_2$	3142	3043	2954	2902, 2867	2046	1593	1487, 1435	1165	451	383(33500), 465(32500)

Table 3. ^{1}H NMR Spectral Data of the Ligand and its Mercury Schiff Base Complexes in DMSO-d_6

Compound	^{1}H NMR data (δ, ppm)
Ligand	7.97 (d, $2H_{d,d'}$, J = 9 Hz), 7.34 (d, $4H_{g,g'}$, J = 8.4 Hz), 6.92 (d, $2H_{f,f'}$, J = 15.9 Hz), 6.66 (d, $4H_{h,h'}$, J = 8.4), 6.60 (dd, $2H_{e,e'}$, J = 7.5 Hz, 9 Hz), 3.47 (t, $4H_{b,b'}$, J = 6 Hz, 4.8 Hz), 2.94 (s, $12H_{i,i'}$), 2.83 (s, $1H_a$), 2.72 (t, $4H_{c,c'}$, J = 4.8 Hz, 6.6 Hz)
$HgLCl_2$	8.28 (d, $2H_{d,d'}$, J = 8.4 Hz), 7.44 (d, $4H_{g,g'}$, J = 8.4 Hz), 7.31 (dd, $2H_{e,e'}$, J = 15.6 Hz, 15.6 Hz), 7.10 (d, $2H_{f,f'}$, J = 15.9 Hz), 6.75 (d, $4H_{h,h'}$, J = 8.4), 3.62 (bt, $4H_{b,b}$), 2.97 (m, $12H_{i,i'}$, $4H_{c,c'}$), 2.74 (bs, $1H_a$).
$HgLBr_2$	8.23 (d, $2H_{d,d'}$, J = 8.1 Hz), 7.43 (d, $4H_{g,g'}$, J = 8.1 Hz), 7.21 (dd, $2H_{e,e'}$, J = 11.1 Hz, 15.3 Hz), 7.05 (d, $2H_{f,f'}$, J = 15.6 Hz), 6.75 (d, $4H_{h,h'}$, J = 8.4), 3.61 (bt, $4H_{b,b}$), 2.97 (m, $12H_{i,i'}$, $4H_{c,c'}$), 2.74 (bs, $1H_a$).
$HgLI_2$	8.23 (bs, $2H_{d,d'}$), 7.58 (dd, $2H_{e,e'}$, J = 4.8 Hz, 12 Hz), 7.41 (d, $4H_{g,g'}$, J = 8.4 Hz), 7.06 (bs, $2H_{f,f'}$), 6.75 (d, $4H_{h,h'}$, J = 8.4 Hz), 3.62 (bt, $4H_{b,b}$), 2.97 (s, $12H_{i,i'}$), 2.89 (bt, $4H_{c,c'}$), 2.78 (bs, $1H_a$).
$HgL(SCN)_2$	8.37 (d, $2H_{d,d'}$, J = 8.4 Hz), 7.61 (d, $4H_{g,g'}$, J = 8.1 Hz),7.19 (d, $2H_{e,e'}$, J = 15.6 Hz), 6.93 (d, $2H_{f,f'}$, J = 9 Hz), 6.74 (d, $4H_{h,h'}$, J = 11.1 Hz), 3.66 (bt, $4H_{b,b}$), 2.97 (m, $4H_{c,c'}$, $12H_{i,i'}$), 2.80 (bs, $1H_a$).
$HgL(N_3)_2$	8.41 (d, $2H_{d,d'}$, J = 7.2 Hz), 7.48 (d, $4H_{g,g'}$, J = 7.2 Hz), 7.23 (d, $2H_{f,f'}$, J = 15.6 Hz), 6.88 (dd, $2H_{e,e'}$, J = 15 Hz, 15.3 Hz), 6.70 (d, $4H_{h,h'}$, J = 7.2), 3.65(bt, $4H_{b,b}$), 2.96 (m, $4H_{c,c'}$, $12H_{i,i'}$), 2.73 (bs, $1H_a$).

Table 4. ^{13}C NMR Spectral Data of the Ligand and its Mercury Schiff Base Complexes in DMSO-d_6

Compound	^{13}C NMR data (δ, ppm)
Ligand	164.11 ($C_{3,3'}$), 151.22 ($C_{9,9'}$), 142.32 ($C_{5,5'}$), 131.12 ($C_{7,7'}$), 128.95 ($C_{6,6'}$), 123.56 ($C_{4,4'}$), 112.39 ($C_{8,8'}$), 60.89 ($C_{1,1'}$), 50.02 ($C_{2,2}$), 40.70 ($C_{10,10'}$)
$HgLCl_2$	167.52 ($C_{3,3'}$), 151.86 ($C_{9,9'}$), 146.05 ($C_{5,5'}$), 129.58 ($C_{7,7'}$), 123.09 ($C_{6,6'}$), 121.64 ($C_{4,4'}$), 112.42 ($C_{8,8'}$), 55.71 ($C_{1,1'}$), 49.28 ($C_{2,2}$), 40.48 ($C_{10,10'}$)
$HgLBr_2$	166.58 ($C_{3,3'}$), 151.74 ($C_{9,9'}$), 144.98 ($C_{5,5'}$), 129.53 ($C_{7,7'}$), 123.30 ($C_{6,6'}$), 122.17 ($C_{4,4'}$), 112.44 ($C_{8,8'}$), 56.70 ($C_{1,1'}$), 49.79 ($C_{2,2}$), 40.48 ($C_{10,10'}$)
$HgLI_2$	166.10 ($C_{3,3'}$), 151.75 ($C_{9,9'}$), 144.76 ($C_{5,5'}$), 129.28 ($C_{7,7'}$), 123.30 ($C_{6,6'}$), 121.95 ($C_{4,4'}$), 112.48 ($C_{8,8'}$), 56.20 ($C_{1,1'}$), 50.18 ($C_{2,2}$), 40.23 ($C_{10,10'}$)
$HgL(SCN)_2$	166.64 ($C_{3,3'}$), 152.00 ($C_{9,9'}$), 147.40 ($C_{5,5'}$), 137.60 (C_{NCS}), 131.12 ($C_{7,7'}$), 122.82 ($C_{6,6'}$), 120.85 ($C_{4,4'}$), 112.30 ($C_{8,8'}$), 56.55 ($C_{1,1'}$), 49.70 ($C_{2,2}$), 40.77 ($C_{10,10'}$)
$HgL(N_3)_2$	168.02 ($C_{3,3'}$), 152.04 ($C_{9,9'}$), 147.57 ($C_{5,5'}$), 129.89 ($C_{7,7'}$), 122.64 ($C_{6,6'}$), 120.54 ($C_{4,4'}$), 112.35 ($C_{8,8'}$), 54.65 ($C_{1,1'}$), 48.90 ($C_{2,2}$), 40.89 ($C_{10,10'}$)

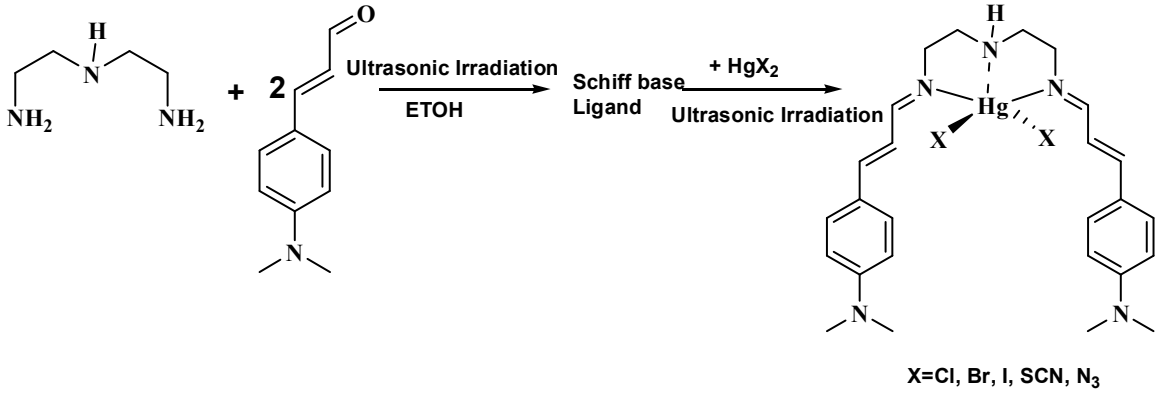

Scheme 2. Synthesis of nanostructured mercury complexes

mercury salts with the neutral NNN donor tridentate Schiff base ligand were synthesized and characterized. Physical and analytical characteristics of the ligand and its new mercury complexes have been tabulated as Table 1. The mercury(II) complexes were readily obtained in good yield on reacting of mercury salt with Schiff base ligand in 1:1 molar ratio. The ligand was obtained in 87% yields, while the yields of its mercury complexes were evaluated in 54 to 91%. The synthesized complexes are insoluble in water, methanol and ethanol but low soluble in CH_2Cl_2 and $CHCl_3$ and are soluble in DMF and DMSO. The ligand and all resultant complexes were colored. The molar conductance values of 10^{-3} M solutions of all compounds in DMF were found in the range of 13.56-23.90 $cm^2\ \Omega^{-1}\ M^{-1}$ at room temperature demonstrating non-electrolytes nature for the mercury complexes [40,41].

IR Spectra

The main infrared absorption peaks for vibration in the structure of the free Schiff base ligand and its mercury complexes in the range of 4000-400 cm^{-1} are summarized in Table 2. All FT/IR spectra of the ligand and its mercury complexes are found in supplementary file as Figs.1S-6S. In the spectrum of ligand, the lack of the characteristic stretching vibrations of C=O of 4,4-dimethylamino-cinnamaldehyde at 1661 cm^{-1} and NH_2 groups of diethylenetriamine at 3336 cm^{-1} confirms formation of Schiff base ligand [32,42]. In IR spectrum of the tridentate ligand appeared a new strong absorption frequency in 1603 cm^{-1} related to stretching vibration of azomethine functional groups, ν(C=N), that confirms successful condensation reaction of starting materials [42,43]. This absorption frequency is found to be shifted towards lower wavenumbers in all complexes that indicates the involvement of the azomethine nitrogens in binding to mercury(II) ions. This suggestion is also confirmed by the existence of a weak vibration at 400-450 cm^{-1} region of complexes spectra assigned to M-N bond stretching vibration [44]. The weak absorption frequencies in IR spectrum of ligand at 3028, 2918, 2881 and 2803 cm^{-1} were attributed to the stretching vibrations of olefinic, aliphatic and iminic C-H bonds, respectively. These vibrations after coordination of ligand to the mercury(II) center is observed at higher frequencies in all complexes spectra. Participation of the secondary amine nitrogen in binding to the mercury center was supported by shift of the stretching vibration peak related to its N-H vibration at 3299 cm^{-1} in the free ligand to lower frequencies in the IR spectra of the synthesized complexes [37]. In addition, the IR spectra of $HgL(N_3)_2$ and $HgL(NCS)_2$ showed new strong peaks at 2046 cm^{-1} and 2107 cm^{-1} related to the coordinated azide and *S*-thiocyanate vibrations [45,46].

UV-Vis Spectra

The electronic spectra of the ligand and its Hg(II) complexes in DMF were recorded at room temperature in the range of 200-700 nm (Fig. 1), and the maximum absorption wavelengths and molar absorption coefficients (ε) are found in Table 2. The electronic spectrum of free

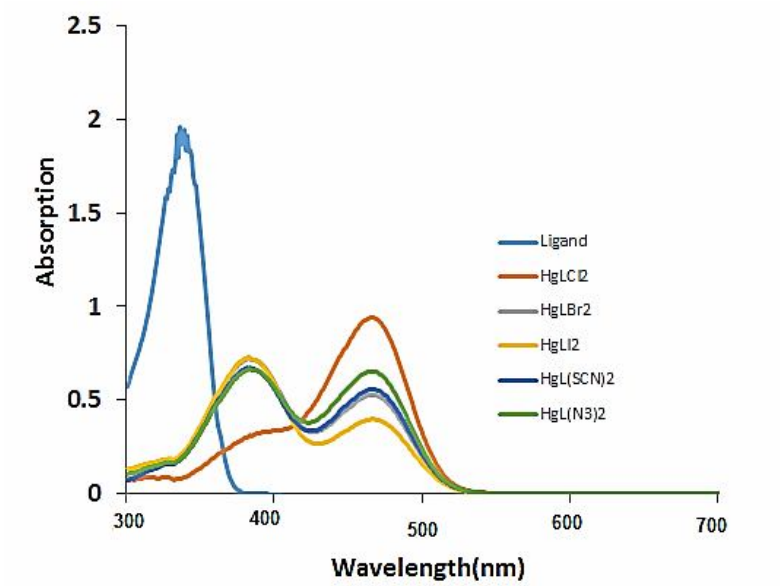

Fig. 1. The electronic spectra of the ligand and its mercury complexes.

ligand showed an internal electronic transition at 335 nm assigning to π-π* electronic transition of benzene rings and azomethine chromophore [25,32,42,47]. In the electronic spectra of mercury complexes, coordination of ligand to metal center influenced on its intensity and location so that it shifts toward the higher wavelength and appears as two completely separated bands assigned to π-π* electronic transition of benzene rings and π-π* electronic transitions of azomethine chromophore, respectively. In electronic spectra of the mercury(II) complexes, since electronic configuration metal ion is d^{10}, the d-d electronic transition bands are not observed and the bands of charge transfer transition (MLCT) were also not appeared probably due to its overlap with π-π* electronic transitions of Schiff base ligand. These considerable changes in electronic spectral of the complexes with respect to the free ligand well support its coordination to mercury ion *via* azomethine nitrogens [31].

^{1}H and ^{13}C NMR of the Schiff Base Ligand and its Mercury Complexes

NMR spectral data of the free ligand and its mercury complexes in DMSO-d_6 solvent can be found in Table 3 and 4 based on Scheme 1. The ^{1}H and ^{13}C NMR spectra of Schiff base ligand and its complexes are compatible with the proposed molecular structures in Scheme 1. ^{1}H NMR spectrum of ligand showed a doublet peak at 7.97 ppm with a coupling constant of 9.0 Hz for azomethine hydrogens of d, d′ due to coupling with hydrogens of e and e′ [48]. The ^{1}H NMR peaks of the azomethine groups in the Hg(II) complexes shift to downfield region and appear in the range of 8.23-8.41 ppm confirming coordination of the ligand to mercury ion *via* iminic nitrogens [25-28,43,47,48]. In the spectrum of the ligand, the signal of $H_{g,g'}$ appeared at 7.34 ppm with coupling constant of 8.40 Hz due to coupling with hydrogens of h and h′. A doublet signal with coupling constant of 15.9 Hz appeared at 6.92 ppm due to coupling hydrogens of f and f′ with hydrogens of e and e′. These signals shift to downfielded regions in all Schiff base complexes. In the ^{1}H NMR spectrum of the free ligand, hydrogen atoms of h, h' appeared as doublet at 6.66 ppm with coupling constant of 8.4 Hz due to coupling with hydrogens of g and g′ that after coordination shifted to weaker fields. A doublet of doublet peak appeared at 6.60 ppm and is surely ascribed to hydrogens of e and e′ with coupling constants of 15.9 Hz and 9.0 Hz due to coupling with hydrogens of d, d′ and f, f′, respectively. This peak shifts toward downfielded regions in all the complexes. For free ligand, two the triplet peak at 3.47 and

2.72 ppm are attributed to aliphatic hydrogens of b, b′ and c, c′ due to coupling with hydrogens of c, c′ and b, b′, respectively. These signals shift toward downfielded area in the Hg(II) complexes spectra. The singlet peaks at 2.94 and 2.83 ppm in the ligand spectrum are attributed to aliphatic hydrogens and secondary amine hydrogen of i, i′ and a, and they appear as downfielded and upfielded peaks in the complexes spectra, respectively. In the ^{13}C NMR spectrum of the ligand ten peaks are observed because of symmetrical structure of Schiff base ligand. The signal at 164.11 ppm in the free ligand spectrum exhibited azomethine carbons ($C_{3,3'}$) as functional group. After coordination, this signal shifts to downfielded region in all the synthesized complexes spectra that confirms coordination of the iminic nitrogens to central metal ion. In the ^{13}C NMR spectrum of the ligand, the peak at 151.22 ppm can be assigned to $C_{9,9'}$. This peak is shifted to 151.74-152.04 ppm in the mercury complexes spectra. The signal at 142.32 ppm in spectrum of the ligand is attributed to $C_{5,5'}$. This signal after coordination is deshielded and shift to downfielded region in all complexes spectra. The signal observed at 131.12 ppm was ascribed to $C_{7,7'}$ that shifts to upfielded region in all complexes spectra except for $HgL(SCN)_2$ that does not change. The signal appeared at 128.95 is assigned to aromatic carbons of $C_{6,6'}$, that is observed at range 122.64-123.30 ppm in the mercury complexes spectra. In ^{13}C NMR spectrum of the free ligand, carbon signal for $C_{4,4'}$ appears at 123.56 ppm that is observed in the range of 120.54-122.17 ppm in the mercury complexes spectra. The peak appeared at 112.39 refers to $C_{8,8'}$ carbons that was observed as downfielded signals in $HgLCl_2$, $HgLBr_2$ and $HgLI_2$, and as upfielded signals in $HgL(NCS)_2$ and $HgL(N_3)_2$ spectra. The signal observed at 60.89 ppm is ascribed to $C_{1,1'}$ carbons that shielded and shifted to strong fields in the mercury complexes spectra. Two peaks found at 50.02 and 40.70 ppm are assigned to aliphatic carbons of $C_{2,2'}$ and $C_{10,10'}$, respectively that are observed at range of 48.90-50.18 ppm and 40.23-40.89 ppm in spectra of the mercury complexes. In addition to the mentioned signals, the signal observed at 137.60 ppm in the mercury thiocyanate complex refers to carbon of coordinated *S*-thiocyanato ligand (C_{SCN^-}).

XRD and SEM Analyses

XRD patterns recorded for nano-powder of the mercury complexes in the 2θ range of 0°-90° are exhibited in Fig. 2. The average particle sizes of the mercury complexes were evaluated using Sherrer's formula from the broad XRD peak ($D = k\lambda/\beta Cos\theta$, where D is the average grain size, k is Blank's constant (0.891), λ is the X-ray wavelength, and θ and β are the diffraction angle and full-width at half maximum of an observed peak, respectively) [49]. The average sizes of the particles for mercury chloride, iodide, thiocyanate and azide were evaluated and found to be about 54.30, 28.49, 55.92, 61.85 nm, respectively. The evaluated data based on XRD patterns confirmed the nano structured size for the mercury complexes. SEM images of mercury complexes have been also presented in Fig. 3 to show the surface morphology of nano-structured compounds. The images showed that the nano-particles are agglomerated and morphologies of prepared nano structured compounds are similar in solid state.

Thermal Investigation

Thermal analyses are generally based on the changes in weight of the material *versus* temperature or time [32,50]. In continue of other investigation, thermal stability of ligand and its complexes were investigated by thermo-gravimetric analyses (TG/DTG/DTA) in the temperature range of room temperature to 1000 °C with the heating rate of 10 (°C min^{-1}) under N_2 atmosphere. As typical ones, TG/DTA/DTG plots of the ligand, $HgLCl_2$ and $HgL(N_3)_2$ complexes are shown in Fig. 4 and the others are found as Figs. 7S-9S in supplementary file associated with this article. Thermo-gravimetric data including thermal decomposition ranges, mass loss (%) and thermokinetics activation parameters of each thermal decomposition step of the ligand and mercury complexes have been tabulated as Tables 5 and 6. The TG/DTA/DTG plots of the ligand and its mercury complexes indicate that ligand is completely eliminated during two thermal stages, while thermal decomposition of the mercury complexes occurs *via* 3-5 thermal steps. According to the thermogravimetric plots (TG/DTA/DTG), it is often possible to search whether there is any coordinated or lattice water in the complexes [51,52]. A mass loss in the range of 50-200 °C for mercury complexes may be due to the existence of adsorbed water molecule [32]. All the titled complexes, except mercury thiocyanate complex, are entirely decomposed.

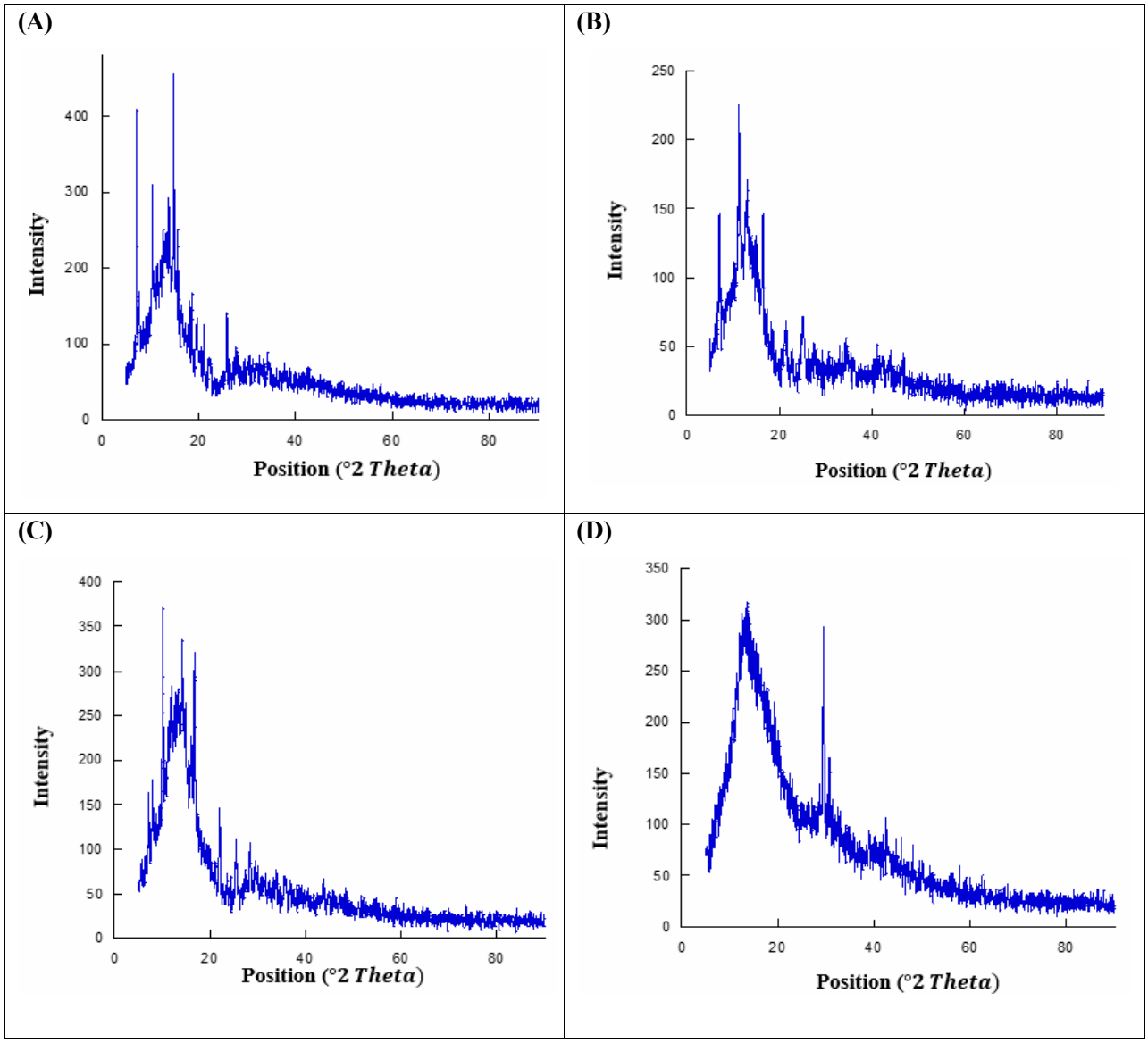

Fig. 2. XRD patterns of mercury chloride (A), iodide (B), thiocynate (C) and azide (D) complexes.

Accordingly thermogravimetric plot of mercury thiocyanate complex consists of four thermal steps for decomposition, and a trace of mercury salt remain at final step. Furthermore, some thermo-kinetics activation parameters of decomposition processes of the ligand and its complexes such as enthalpy (ΔH*), entropy (ΔS*), Gibbs free energy (ΔG*), Arrhenius constant (A) and activation energy (ΔE*) were estimated using Coats-Redfern equation [53,54] based on the TG/DTG data of compounds and were summarized in Table 6. Activation parameters of the ligand and its mercury complexes may indicate the thermal stability of them. As seen in Table 6, the activation energies (E*) in the different steps of thermal decomposition processes are evaluated in the span of 16.36-313.11 kJ mol^{-1} indicating the suitable thermal stability for the compounds. The values of the activation entropy (ΔS*) are evaluated as

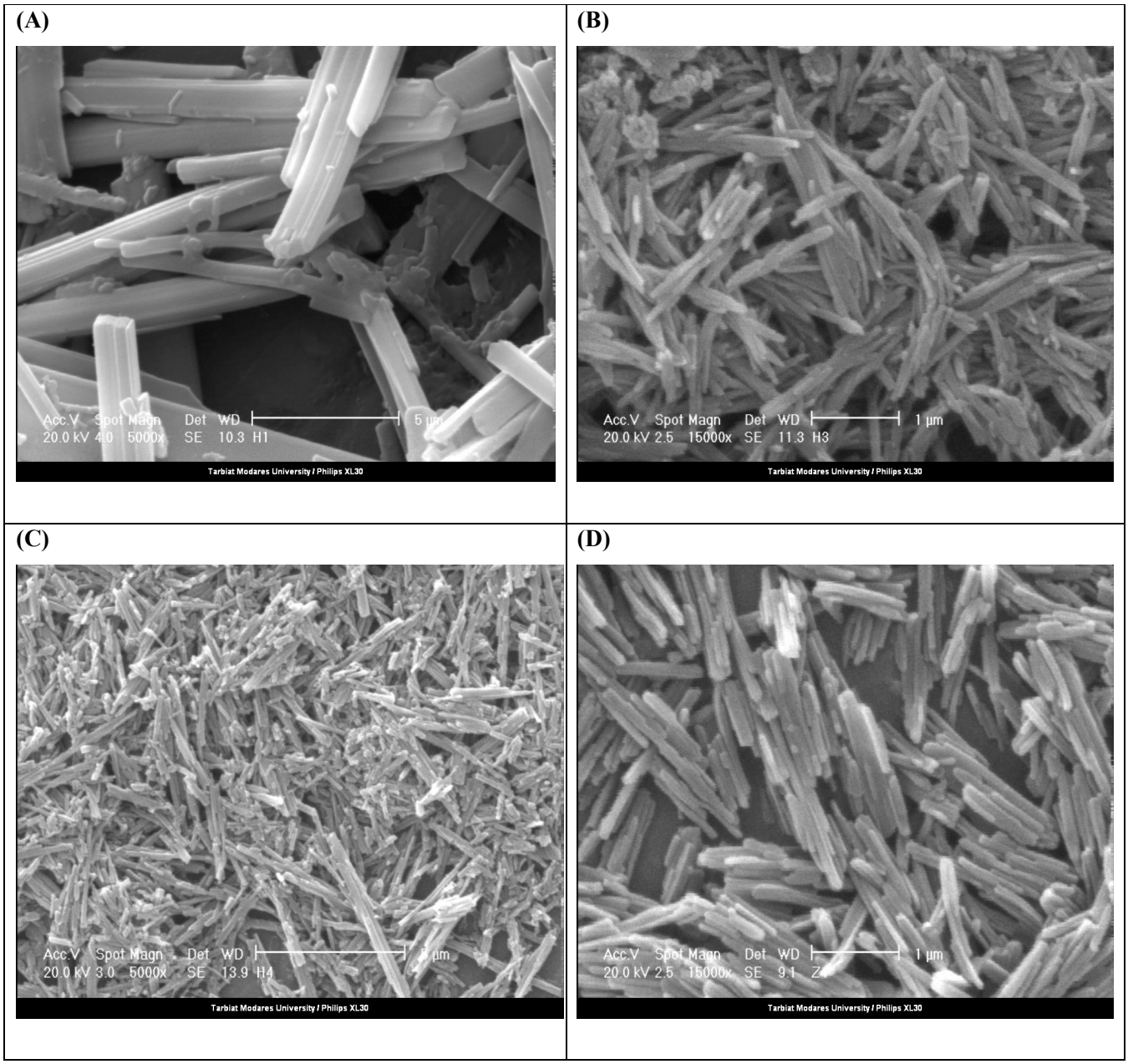

Fig. 3. SEM images of mercury chloride (A), iodide (B), thiocyanate (C) and azide (D) complexes.

negative numbers for all thermal decomposition steps of the compounds except for the first step of thermal decomposition of the mercury complexes. The negative values indicate an associated mechanism at rate determining step of thermal decomposition process and positive value of the activation entropy (ΔS^*) suggest a normal pathway for thermal decomposition process [35,55]. Relatively high values for the activation enthalpy (ΔH^*) and Gibbs free energy (ΔG^*) indicate the endothermic and not-spontaneous character for all thermal decompositions steps and therefore the suitable stability for them.

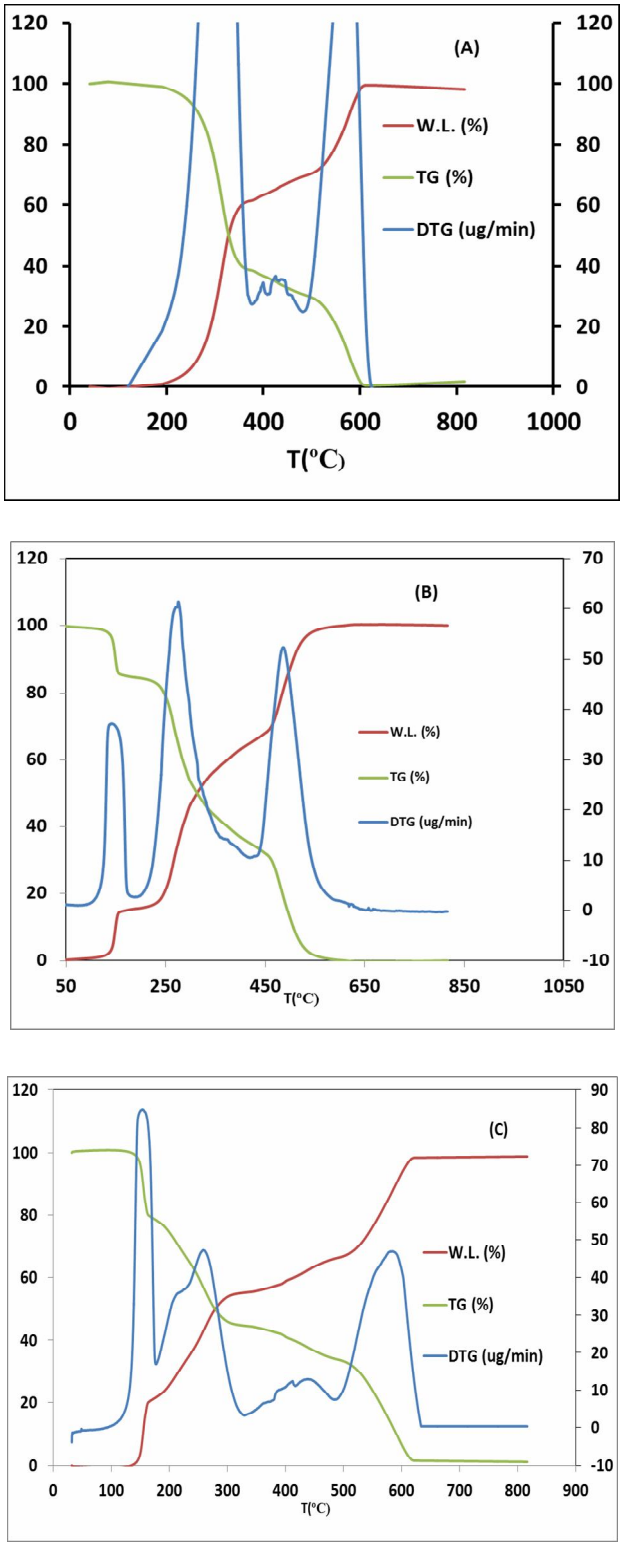

Fig. 4. TG/DTG/DTA plots of Ligand (A), $HgLCl_2$ (B) and $HgL(N_3)_2$ (C) complexes.

Table 5. Thermal Analyses Data of the Ligand and its Mercury Complexes Including Temperature Range, Differential Thermal Gravimetric Peak (DTG), Mass Loss%, Proposed Segment and Final Residuals

Compound	Temperature range (°C)	Mass loss (%) found (Calculated)	DTG peak (°C)	Proposed segment	Final residue
Ligand	190-430	65.55 (63.79)	317	$C_{18}H_{22}N_2$	-
	430-816	34.03 (36.21)	582	$C_8H_{13}N_3$	
$HgLCl_2$	83-193	15.48 (15.47)	153	H_2O	$C_{26}H_{35}Cl_2HgN_5$
	193-424	49.80 (51.22)	280	$C_{26}H_{35}N_5$	$HgCl_2$
	424-816	34.67 (33.30)	491	$HgCl_2$	-
$HgLBr_2$	87-176	7.10 (7.73)	147	H_2O	$C_{26}H_{35}Br_2HgN_5$
	176-273	17.08 (16.61)	255	$C_8H_{14}N_2$	$C_{18}H_{21}Br_2HgN_3$
	273-445	32.89 (33.58)	307	$C_{18}H_{21}N_3$	$HgBr_2$
	445-581	27.09 (27.16)	527	$Hg_{0.33}Br_2$	$Hg_{0.67}$
	581-817	12.63 (16.15)	61	$Hg_{0.67}$	-
$HgL(SCN)_2$	92-167	7.10 (6.90)	150	H_2O	$C_{28}H_{35}HgN_7S_2$
	167-393	56.61 (56.66)	297	$C_{26.5}H_{35}N_{5.5}S_{0.5}$	$C_{1.5}HgN_{1.5}S_{1.5}$
	393-505	7.75 (7.37)	444	NCS	$C_{0.5}HgN_{0.5}S_{0.5}$
	505-816	23.76 (24.04)	614	$C_{0.5}HgN_{0.5}S_{0.5}$	A trace of mercury salt
$HgL(N_3)_2$	78-179	21.79 (22.01)	161	H_2O	$C_{26}H_{35}HgN_{11}$
	179-333	33.61 (33.92)	267	$C_{21}H_{25}N_2$	$C_5H_{10}HgN_9$
	333-488	10.73 (10.90)	426	$C_5H_{10}N_2$	HgN_7
	488-816	32.70 (33.17)	594	HgN_7	-

Antimicrobial Activity

Antimicrobial activity of the Schiff base ligand and its mercury complexes were tested *in vitro* against four bacteria including *E. coli* and *P. aeruginosa* as Gram-negative bacteria; *S. aureus* and *B. subtilis* as Gram-positive bacteria and two funguses including *C. albicans* and *A. oryzae* by using well diffusion method and zones of growth inhibition (mm) of the bacteria and fung uses growth as antimicrobial activities have been collected in Tables 7 and 8.

Antimicrobial activities of compounds have been investigated in three concentrations (15, 7.5 and/or 3.75 mg mL^{-1}) and it was found that as the concentration increased, the activity also increased. Antimicrobial data showed that the Schiff base ligand and its mercury complexes have well activity against chosen bacteria and funguses, and also it was cleared that the mercury complexes have higher activity as compared with their parent Schiff base ligand under similar test conditions,

Table 6. Thermo-kinetic Parameters of the Thermal Decomposition Steps of the Ligand and its Mercury Complexes

Compound	Decomposition step (°C)	E* (kJ mol^{-1})	A* (1 s^{-1})	ΔS* (kJ mol^{-1} K^{-1})	ΔH* (kJ mol^{-1})	ΔG* (kJ mol^{-1})
Ligand	190-430	101.94	2.88×10^{6}	-1.27×10^{2}	97.03	1.72×10^{2}
	430-816	145.03	2.97	-2.45×10^{2}	137.92	3.47×10^{2}
$HgLCl_2$	83-193	193.62	1.01×10^{22}	1.73×10^{2}	190.07	1.16×10^{2}
	193-424	48.97	6.28×10^{1}	-2.16×10^{2}	44.37	1.64×10^{2}
	424-81	50.72	5.30×10^{0}	-2.39×10^{2}	44.36	2.27×10^{2}
$HgLBr_2$	87-176	59.03	2.12×10^{5}	-1.46×10^{2}	55.53	1.17×10^{2}
	176-273	80.83	4.35×10^{5}	-1.42×10^{2}	76.44	1.51×10^{2}
	273-445	33.03	1.04×10^{00}	-2.50×10^{2}	28.20	1.73×10^{2}
	445-581	70.42	9.28×10^{1}	-2.15×10^{2}	63.77	2.36×10^{2}
	581-817	77.08	1.69×10^{2}	-2.11×10^{2}	69.71	2.57×10^{2}
$HgL(SCN)_2$	92-167	313.11	9.50×10^{36}	4.60×10^{2}	309.60	1.15×10^{2}
	167-393	41.02	8.31×10^{00}	-2.33×10^{2}	36.27	1.69×10^{2}
	393-505	36.91	1.40×10^{00}	-2.49×10^{2}	30.95	2.10×10^{2}
	505-816	94.01	1.05×10^{3}	-1.96×10^{2}	86.63	2.61×10^{2}
$HgL(N_3)_2$	78-179	236.74	6.36×10^{26}	2.65×10^{2}	233.12	1.18×10^{2}
	179-333	43.08	4.25×10^{1}	-2.19×10^{2}	38.59	1.57×10^{2}
	333-488	16.36	4.31×10^{-2}	-2.78×10^{2}	10.55	2.05×10^{2}
	488-816	112.01	2.13×10^{4}	-1.71×10^{2}	104.80	2.53×10^{2}

that this can be explained based on Overtone's concept and Tweedy's chelation theory [56,57]. The cell membrane is sensitive and permeable only for lipid-soluble substances. The antimicrobial activity of a compound is pertained on its lipophilicity character. After complexation, the lipophilicity of complexes is increased because the polarity of the metal ion significantly is reduced because of overlap of its valence orbitals with the ligand orbitals. This factor causes π-electron delocalization over whole of the ligand chelating ring and positive charge of metal ion is decreased. As a result, increase in lipophilicity character of the complexes leads to facilitating their diffusion into microorganism cell wall and blocking active sites of bacteria and/or fungi enzymes leading to prevents their growth leading to death. In the case of antibacterial studies, it was found that the mercury chloride and azide complexes have the largest effect against *Pseudomonas aeruginosa* and *Bacillus subtilis*, respectively. Based on the summarized data in Table 7, $HgLCl_2$ complex showed the most antibacterial activity against *Escherichia coli*. The antibacterial activities of the mercury complexes against *Staphylococcus aureus* can be ordered as following trend:

Table 7. Antibacterial Activity of the Ligand and its Mercury Complexes as Diameter of Zone of Inhibition (mm) around the Wells (Filled with 15, 7.5 and/or 3.75 mg mL^{-1})[a]

Compound	Gram-positive						Gram-negative					
	Bacillus subtilis			*Staphylococcus aureus*			*Pseudomonas aeruginosa*			*Escherichia coli*		
	15[a]	7.5[a]	3.75[a]	15	7.5	3.75	15	7.5	3.75	15	7.5	3.75
Ligand	16.0	14.3	13.3	14.2	11.0	10.5	13.6	9.5	9.5	17.3	15.6	11.0
$HgLCl_2$	30.0	31.0	28.5	6.0	6.0	6.0	35.5	33.8	33.7	28.0	27.0	27.0
$HgLBr_2$	29.3	26.7	26.5	25.0	23.6	23.6	33.0	30.0	30.0	26.0	25.0	25.0
$HgLI_2$	27.6	26.0	24.5	19.0	18.0	18.0	31.0	31.0	31.0	25.0	24.3	23
$HgL(SCN)_2$	23.0	22.0	21.0	20.5	18.5	17.5	32.6	27.0	25.0	23.0	21.6	19.0
$HgL(N3)_2$	36.0	32.4	28.0	6.0	6.0	6.0	33.3	30.6	30.6	27.6	24.5	24.4

Table 8. Antifungal Activity of the Ligand and its Mercury Complexes as Diameter of Zone of Inhibition (mm) around the Wells (Filled with 15, 7.5 and/or 3.75 mg mL^{-1})[a]

Compound	*Candida albicans*			*Aspergillus orayzea*		
	15[a]	7.5[a]	3.75[a]	15	7.5	3.75
Ligand	16.4	14.3	13.0	6.00	6.00	6.00
$HgLCl_2$	33.3	32.4	22.0	28.1	25.0	19.8
$HgLBr_2$	30.0	30.2	28.0	6.0	6.0	6.0
$HgLI_2$	28.0	27.0	26.5	24.2	24.0	23.0
$HgL(SCN)_2$	24.5	24.3	24	6.9	6.0	6.0
$HgL(N_3)_2$	35.0	32.3	31.3	24.4	24.3	21.0

$HgLBr_2$ > $HgL(NCS)_2$ > $HgLI_2$ > $HgLCl_2$ ~ $HgL(N_3)_2$ > ligand

In antifungal investigation it was found that $HgL(N_3)_2$ and $HgL(SCN)_2$ complexes have the maximum and minimum activity against *Candida albicans* respectively. As seen in Table 8, the mercury chloride complex was more active against *Aspergillus orayzea* as compared with other compounds.

CONCLUSIONS

In this work, synthesis and spectral characterization of a tridentate Schiff base ligand and its new mercury(II) complexes with the general formula of $HgLX_2$ (X = Cl^-, Br^-, I^-, N_3^- and SCN^-) wer reported. The spectral data supported that the ligand is coordinated to mercury ions as tridentate ligand. Also, the nanostructured forms of some complexes were prepared by using the sonication method. The

morphology and size of nano-structured complexes were characterized by XRD and SEM techniques. TG/DTG/DTA plots revealed that thermal decomposition process of the ligand is completely occurrs during two steps while its mercury complexes are decomposed *via* 3-5 thermal steps from room temperature to 1000 °C. All mercury complexes except the mercury thiocyanate complex that leaves out a trace of mercury salt as final residual, were completely decomposed without any residual. Some activation thermokinetics parameters such as activation energy (E*), enthalpy (ΔH*), entropy (ΔS*) and Gibbs free energy (ΔG*) were calculated using the Coats-Redfern equation based on TG/DTG/DTA plots. These results showed that thermal decomposition character for all compounds is non-spontaneous. Finally, antimicrobial testing of the ligand and its complexes were screened *in vitro* against two Gram-negative and positive bacterial strains and also two fungal strains. The mercury complexes showed more antimicrobial activity than free ligand. Based on well diffusion method, $HgLCl_2$ was found as the most effective complex against two Gram-negative bacteria of *Pseudomonas aeruginosa* and *Escherichia coli* while $HgL(N_3)_2$ and $HgLBr_2$ showed good inhibitory effects against *Bacillus subtilis* and *Staphylococcus aureus* respectively with respect to others. Also, among the compounds, $HgL(N_3)_2$ and $HgLCl_2$ were found to be the best antifungal compounds against *Candida albicans* and *Aspergillus orayzea* respectively.

REFERENCES

[1] N. Raman, S.J. Raja, J. Joseph, J.D. Raja, Russ. J. Coord. Chem. 33 (2007) 7.

[2] H. Temel, S. İlhan, M. Şekerci, Synth. React. Inorg. Met. -Org. Chem. 32 (2002) 1625.

[3] Z.H.A. El-Wahab, O.A. Ali, B.A. Ismail, J. Mol. Struct. 1144 (2017) 136.

[4] W.A. Zoubi, Y.G. Ko, Appl. Org. Chem. 31 (2017) e3574.

[5] F.K. Ommenya, E.A. Nyawade, D.M. Andala, J. Kinyua, J. Chem. Article ID 1745236 (2020) 1.

[6] L. John, R.S. Joseyphus, I.H. Joe, SN Appl. Sci. 2 (2020) 500.

[7] E.M. Zayed, M. Zayed, Spectrochim. Acta Part A, 143 (2015) 81.

[8] S. Farahmand, M. Ghiaci, M. Vatanparast, J.S. Razavizadeh, New J. Chem. 44 (2020) 7517.

[9] D.N. Dhar, C. Taploo, J. Sci. Indust. Res. 41 (1982) 501.

[10] R. Nair, A. Shah, S. Baluja, S. Chanda, J. Serb. Chem. Soc. 71 (2006) 7334.

[11] M. Jesmin, M. Ali, J. Khanam, J. Pharm. Sci. 34 (2010) 1.

[12] A. Jarrahpour, D. Khalili, E.D. Clercq, C. Salmi, J.M. Brunel, Molecules 12 (2007) 1720.

[13] Z. Parsaee, K. Mohammadi, M. Ghahramaninezhad, B. Hosseinzadeh, New J. Chem. 40 (2016) 10569.

[14] S. Ghanbari Niyaky, M. Montazerozohori, R. Naghiha, J. Phys. Orga. Chem. 30 (2017) e3718.

[15] A.K. Starkov, T.N. Zamay, A.A. Savchenko, E.V. Ingevatkin, N.M. Titova, O.S. Kolovskaya, N.A. Luzan, P.P. Silkin, S.A. Kuznetsova, Doklady Biochem. Biophys. 467 (2016) 92.

[16] S.K. Lee, K.W. Tan, S.W. Ng, J. Inorg. Biochem. 159 (2016) 14.

[17] S.N. Pandeya, D. Sriram, G. Nath, E. DeClercq, Euro. J. Pharma. Sci. 9 (1999) 25.

[18] R. Sanyal, S. Kumar Dash, P. Kundu, D. Mandal, S. Roy, D. Dasa, Inorg. Chim. Acta 453 (2016) 394.

[19] H. He, *et al.*, Inorg. Chem. 44 (2005) 7431.

[20] P.L. Lam, G.L. Lu, K.H. Choi, Z. Lin, S.H.L. Kok, K.K.H. Lee, K.H. Lam, H. Li, R. Gambari, Z.X. Bian, W.Y. Wong, C.H. Chui, RSC Adv. 6 (2016) 16736.

[21] S. Ambreen, A. Mohammad, A. Asad, U. Khan, Spectrochim. Acta Part A 79 (2011) 1866.

[22] M. Montazerozohori, S.A. Musavi, A. Masoudiasl, A. Hojjati, A. Assoud, Spectrochim. Acta A 147 (2015). 139.

[23] A. Morsali, M.Y. Masoomi, Coord. Chem. Rev. 253 (2009) 1882.

[24] J.N. LePage, W. Lindner, G. Davies, D.E. Seitz, B.L. Karger, Anal. Chem. 51 (1979) 433.

[25] S.A. Musavi, M. Montazerozohori, A. Masoudiasl, R. Naghiha, S. Joohari, A. Assoud, J. Mol. Struct. 1145 (2017) 65.

[26] M. Montazerozohori, M. Nasr-Esfahani, M. Hoseinpour, A. Naghiha, S. Zahedi, Chem. Spec. Bioavailab. 26 (2014) 240.

[27] J.A. Lemire, J.J. Harrison, R.J. Turner, Nat. Rev.

Microb. 1 (2013) 371.
[28] A. DehnoKhalaji, Gh. Grivani, M. Rezaei, K. Fejfarova, M. Dusek, Polyhedron 30 (2011) 2790.
[29] T.W. Clarkson, L. Magos, Critical Rev. Toxic. 36 (2006) 609.
[30] Z. Zhang, J. Li, X. Song, J. Mac, L. Chen. RSC Adv. 4 (2014) 46444.
[31] M. Montazerozohori, S.A. Musavi, A. Naghiha, S. Veyseh, J. Chem. Sci. 126 (2014) 227.
[32] S. Khani, M. Montazerozohori, R. Naghiha, J. Phys. Org. Chem. 31 (2018) e3873.
[33] M. Habibi, M. Montazerozohori, A. Lalegani, R. Harrington, W. Clegg, Anal. Sci. X-ray Structure Analysis Online 23 (2007) x49.
[34] M. Montazerozohori, M. Sedighipoor, Spectrochim. Acta Part A 96 (2012) 70.
[35] M. Montazerozohori, S. Khani, H. Tavakol, A. Hojjati, M. Kazemi, Spectrochim. Acta Part A: 81 (2011) 122.
[36] M. Montazerozohori, S.A. Musavi, J. Coord. Chem. 61 (2008) 3934.
[37] M. Montazerozohori, A. Masoudiasl, Th. Doert, H. Seykens, RSC Adv. 6 (2016) 21396.
[38] M. Montazerozohori, A. Nazaripour, A. Masoudiasl, R. Naghiha, M. Dusek, M. Kucerakova, Mater. Sci. Engin. C 55 (2015) 462.
[39] A. Abou-Hussein, W. Linert, Spectrochimica Acta Part A 141 (2015) 223.
[40] U. Rabie, A. Assran, M. Abou-El-Wafa, J. Mol. Struct. 872 (2008) 113.
[41] Y. Harinath, D. Harikishore Kumar Reddy, B. Naresh Kumar, Ch. Apparao, K. Seshaiah, Spectrochim. Acta Part A 101 (2013) 264.
[42] M. Montazerozohori, S. Mojahedi Jahromi, A. Masoudiasl, P. McArdle, Spectrochim. Acta Part A 138 (2015) 517.
[43] M. Montazerozohori, S.M. Jahromi, A. Naghiha, J. Ind. Eng. Chem. 22 (2015) 248.
[44] D.X. West, A.A. Nassar, F.A. El-Saied, M.I. Ayad, Transition Met. Chem. 24 (1999) 617.
[45] L.K. Das, R.M. Kadam, A. Bauzá, A. Frontera, A. Ghosh, Inorg. Chem. 51 (2012) 12407.
[46] S. Das, K. Bhar, S. Chattopadhyay, P. MitrabVincent, J. Smith, L.J. Barbour, B.K. Ghosh, Polyhedron 38 (2012) 26.
[47] A. Masoudiasl, M. Montazerozohori, R. Naghiha, A. Assoud, P. McArdle, M. Safi Shalamzari, Mater. Sci. Eng. C 61 (2016) 809.
[48] H. Ünver, Z. Hayvali, Spectrochim. Acta Part A 75 (2010) 782.
[49] J. Yang, C. Lin, Z. Wang, J. Lin, Inorg. Chem. 45 (2006) 8973.
[50] D.R. Trivedi, P. Dastidar, Crystal Growth & Design 6 (2006) 2114.
[51] H. Cesur, T.K. Yazicilar, B. Bati, V.T. Yilmaz, Synth. React. Inorg. Met. -Org. Chem. 31 (2001) 1271.
[52] S.A. Sallam, Trans. Met. Chem. 30 (2005) 341.
[53] A.W. Coats, J. Redfern, Nature 201 (1964) 68.
[54] S. Sen, P. Talukder, G. Rosair, S. Mitra, Struct. Chem. 16 (2005)605.
[55] T.M. Ismail, A.A. Saleh, M.A. El Ghamry, Spectrochimica Acta Part A 86 (2012) 276.
[56] B. Tweedy, Phytopathology 55 (1964) 910.
[57] J.W. Searl, R. Smith, S. Wyard, Proceed. Phys. Soc. 78 (1961) 1174.